Synthesis of a highly recoverable 3D MnO₂/rGO hybrid aerogel for efficient adsorptive separation of pharmaceutical residue

Billie Yan Zhang Hiew[1], *Wan Ting Tee*[1], *Nicholas Yung Li Loh*[1,2],
Kar Chiew Lai[1], *Svenja Hanson*[2], *Suyin Gan*[1],
Suchithra Thangalazhy-Gopakumar[1], *Lai Yee Lee*[1,*]

[1] *Department of Chemical and Environmental Engineering, University of Nottingham Malaysia, Jalan Broga, 43500 Semenyih, Selangor Darul Ehsan, Malaysia.*
[2] *Department of Chemical and Environmental Engineering, University of Nottingham Ningbo China, Ningbo 315100, China.*

ARTICLE INFO

ABSTRACT

Water contamination by non-steroidal anti-inflammatory drugs, such as acetaminophen, is an emerging ecological concern. In this study, a new three-dimensional manganese dioxide-engrafted reduced graphene oxide (3D MnO₂/rGO) hybrid aerogel was developed for acetaminophen sequestration. The synthesis involved firstly the self-assembly of GO aerogel, followed by thermal reduction and *in-situ* MnO₂ growth by redox-reaction. The aerogel demonstrated interlinked planes with smooth surfaces deposited with MnO₂ nanospheres and pores of 138.4 – 235.3 μm width. The influences of adsorbent dosage, initial pH, acetaminophen concentration, temperature and contact time were investigated. It was determined that the adsorption of acetaminophen occurred on uniform sorption sites in the aerogel, as suggested by the best fit of data to the Langmuir isotherm, yielding a maximum adsorption capacity of 252.87 mg/g. This highest adsorption performance of the 3D MnO₂/rGO aerogel was attained at a dosage of 0.6 g/L, initial pH of 6.2 and temperature of 40°C. The process kinetics were in-line with the pseudo-first-order and pseudo-second-order kinetics at 10 and 20 – 500 mg/L concentrations, respectively. Thermodynamic assay showed the spontaneity and endothermicity features of the 3D MnO₂/rGO-acetaminophen system. The acetaminophen adsorption mechanisms were mainly hydrogen bonding and pore entrapment. Moreover, the as-synthesised aerogel was effectively regenerated using acetone and re-utilised in four adsorption-desorption cycles. Overall, the results highly recommend the implementation of the 3D MnO₂/rGO hybrid aerogel for purification of wastewater polluted by acetaminophen residue.

© 2022 The Research Center for Eco-Environmental Sciences, Chinese Academy of Sciences. Published by Elsevier B.V.

---

* Corresponding author.
   E-mail: Lai-Yee.Lee@nottingham.edu.my (L.Y. Lee).

Introduction

Water pollution by pharmaceutical residues is a relatively new environmental issue attracting significant attention worldwide. Among these residues is acetaminophen (N-acetyl-p-aminophenol or paracetamol), an anti-inflammatory drug with antipyretic and analgesic characteristics, which is widely applied for pain and fever management. It is one of the most consumed drugs globally with an estimated annual production of more than 145,000 tonnes (Kekes et al., 2020). Nevertheless, acetaminophen cannot be completely metabolised such that 20% of the medicine is excreted out to the environment as metabolites which include sulphate conjugates, paracetamol cysteinate or mercapturate (Nourmoradi et al., 2018). It is generally a safe medicine for consumption under appropriately administrated dosage. However, an excessive ingestion of acetaminophen can lead to accumulation of reactive benzoquinoneimine (N-acetyl-para-benzoquinoneimine) metabolite (Tortet et al., 2017), consequently causing acute liver failure and nephrotoxicity (Tyszczuk-Rotko et al., 2019). Despite being present in low concentration range (ng/L to µg/L) (Patel et al., 2021), an effective wastewater treatment system is necessary to regulate the acetaminophen concentration in aquatic resources to minimise its negative impacts on both humans and the biosphere.

Adsorption emerges as a versatile and cost effective solution for pharmaceuticals pollution abatement as it is operable under moderate conditions and does not form secondary waste with the re-use of regenerated adsorbent (Mahmoudi et al., 2020). Several adsorbents have been reported to remove acetaminophen with different degrees of efficiency in the literature. For instance, spent tea leaves activated carbon showed an adsorption capacity of 59.2 mg/g for acetaminophen (Wong et al., 2018) while rice husk activated carbon had an adsorption capacity of 50.25 mg/g (Paredes-Laverde et al., 2019). Meanwhile, ozone treated multi-walled carbon nanotubes exhibited 250 mg/g adsorption towards acetaminophen (Yanyan et al., 2018a). A double oxidised graphene oxide developed by Moussavi et al. (2016) adsorbed 704 mg/g of acetaminophen (Moussavi et al., 2016), whereas a Mobil catalytic material encapsulated with reduced graphene oxide (MCM-41-G) sequestered 555.6 mg/g (Akpotu & Moodley, 2018). Among the explored adsorbing substrates, carbon nano-adsorbents demonstrated comparatively high adsorption efficiency towards acetaminophen which could be linked to their ultra-high surface area and chemical functionalities. Despite these remarkable findings, retrieval of nano-sized adsorbents poses several challenges in adsorption applications. Furthermore, leakage of nanomaterials into aquatic systems may create secondary pollution. There are several approaches to recover carbon nanomaterials from the aqueous environment, such as membrane filtration and high speed centrifugation. Alternatively, the carbon nanomaterials can be iron-doped to facilitate their separation from the aqueous body based on their magnetic properties (Gabris et al., 2021).

Two-dimensional (2D) graphene oxide (GO) with exceptional properties has acquired popularity as the precursor for preparation of various three-dimensional (3D) hierarchical graphene configurations such as aerogel, hydrogel and bead.

Assembly of the freestanding GO sheets into 3D macrostructures presents a promising strategy to addressing the constraints of difficult separation and material loss. The 3D graphene architectures could integrate the 2D GO intrinsic properties into the 3D structure, hence improving its feasibility in industrial adsorption applications (Lai et al., 2020). In particular, 3D graphene aerogel has garnered much interest in environmental pollution abatement due to its high specific surface area, porous structure, ample chemical functionalities and extremely low density. For example, it is reported that a 3D pre-treated peanut shell-supported GO aerogel demonstrated 228.83 mg/g adsorption capacity towards norfloxacin (Dan et al., 2020). Other studies have also indicated the potential application of 3D graphene aerogel in pharmaceutical effluent treatment through various adsorption mechanisms which include π-π interaction (Yao et al., 2017), electrostatic attraction (Yu et al., 2017) and hydrophobic interactivity (Shan et al., 2017).

For enhancement of adsorption performance, additional functional groups could be introduced onto the surface of the 3D graphene aerogel by chemical functionalisation, which likely imparts additional sorption sites and increased selectivity for specific pollutants. An efficient and facile way to achieve this is the intercalation of metal oxide such as manganese dioxide (MnO_2) (Minale et al., 2021), titanium dioxide (TiO_2) (Taoufik et al., 2019) and zirconia (ZrO_2) (Zou et al., 2021). MnO_2 was opted for this research due to its unique layered nanostructures in crystal lattices, high specific surface area and environmental friendliness (Hu et al., 2021). The presence of MnO_2 in the 3D graphene aerogel could also facilitate electron transfer mechanism between the functional groups of the pollutant and the MnO_2 surface (Liao et al., 2021). Furthermore, the hydrated cations embedded in MnO_2 could serve as additional functional groups for the adsorption of the pollutant (Jiang et al., 2019). Hence, the implant of MnO_2 into the 3D graphene aerogel offers an opportunity in tailoring microstructures within the adsorbent as well as addition of new chemical functional groups.

In this research, a new 3D reduced GO aerogel engrafted with MnO_2 nanoparticles (3D MnO_2/rGO) was developed for the treatment of wastewater containing acetaminophen. Carmellose sodium (CS) was selected to support the aerogel skeleton as it is a water-soluble polysaccharide biopolymer which binds efficiently with GO in water. Moreover, hydroxyl group of CS could interact with the carboxylic and hydroxyl groups of GO through hydrogen bonding, producing an eco-friendly and non-toxic 3D GO aerogel (Ren et al., 2018). MnO_2 nanoparticles were introduced into the aerogel by *in situ* growth of MnO_2 on the aerogel through redox reaction. To date, there is no available literature on the adsorption of acetaminophen by 3D MnO_2/rGO aerogel. This is the first paper detailing the adsorption performance of this synthesised 3D MnO_2/rGO aerogel toward acetaminophen, along with its regeneration potential and the mechanisms of interactions between the pharmaceutical and the 3D graphene aerogel. The evaluation of adsorption equilibrium and kinetic parameters was carried out to obtain an in-depth understanding of the adsorption system. The practicability of the 3D MnO_2/rGO aerogel was finally examined by a regeneration study.

1. Materials and methods

1.1. Synthesis of 3D graphene aerogel

GO, the precursor for 3D MnO_2/rGO composite synthesis, was firstly prepared according to the altered Hummers formulation. An aqueous suspension of GO (6 mg/mL) was mixed with CS ($C_8H_{16}NaO_8$, 263.2 g/mol, 2 g, Sigma Aldrich, Germany) for 8 hr. The homogeneous suspension was next transferred into a mould and frozen at -20°C for 24 hr, before undergoing lyophilisation in a freeze dryer (Christ Alpha 1-2 LDplus, Germany) operated at -55°C under vacuum condition. The resulting aerogel was then subjected to thermal reduction at 200°C. MnO_2 nanoparticles were engrafted on the rGO aerogel by redox reaction. In detail, 0.8 g of $KMnO_4$ was added into 100 mL of ultrapure water, followed by adjustment of the solution pH to 2 using 0.1 mol/L hydrochloric acid (HCl). Next, 0.3 g of rGO aerogel was immersed in the acidic $KMnO_4$ solution for 1 hr while keeping the temperature of the reacting vessel at 90°C. The reaction was terminated by pouring 10 mL of H_2O_2 (30%) into the reaction vessel. The final product viz. 3D MnO_2/rGO aerogel was rinsed thoroughly for removal of any by-products and dried at 60°C, for 12 hr.

1.2. Characterisation of adsorbent

Field emission scanning electron microscopy (FESEM, Quanta 400F, 20kV, USA) was used to study the surface morphology of the 3D MnO_2/rGO sample. The composition of different elements in the sample was measured by an energy dispersive X-ray detector (EDX, Oxford-Instruments INCA 400, UK). Fourier transform infrared spectroscopy (FTIR, Spectrum RXI Perkin Elmer, USA) was employed to detect the chemical reactive groups existing in the 3D MnO_2/rGO sample. The crystallinity of the 3D MnO_2/rGO was examined by X-ray diffraction (XRD, PANalytical, USA) with CuK radiation source (λ=0.15418 nm) over $7° \leq 2\theta \leq 80°$. The point of zero charge (PZC) of the 3D MnO_2/rGO was determined based on 30 mg of the adsorbent which was agitated in 50 mL potassium nitrate (KNO_3) solutions (0.1 mol/L) of pH varying from 2 – 11. Shaking of the mixtures was performed in a waterbath shaker (Protech, Malaysia) at 30°C and 200 rpm, for overnight.

1.3. Adsorption tests

A 500 mg/L concentration of acetaminophen stock solution was initially prepared by pouring 0.51 g of acetaminophen salt ($C_8H_9NO_2$, 151.165 g/mol, purity > 98%, analytical grade, Sigma Aldrich, Germany) into a volumetric flask containing 1 L ultrapure water. After shaking vigorously, the stock solution was diluted to different working concentrations for use in the subsequent adsorption tests.

The adsorption experiment was performed by contacting a certain mass of 3D MnO_2/rGO in 50 mL acetaminophen solution of known concentration, followed by agitation in the waterbath shaker. The parameters investigated in this study included adsorbent dosage (0.1 – 2 g/L), initial solution pH (2 – 11), initial acetaminophen concentration (10 – 500 mg/L), temperature (30 – 40°C) and contact time (5 – 480 min). The detection of acetaminophen concentration in the sample solution

was carried out using a high-performance liquid chromatography (HPLC, Agilent Technologies, HPLC 1260, USA) attached to an ultra-violet (UV) detector. Prior to the HPLC analysis, the aspirated sample solution (1 mL) was forced to pass through a polytetrafluoroethylene (PTFE) membrane filter (pore size of 0.45 µm, Chromafil, Germany) and finally collected in a screw-neck vial (2 mL). The HPLC column which was used for acetaminophen analysis was a C18 column of 4.6 m x 100 mm in dimension and 3.5 µm pore size (Zorbax Eclipse Plus C18, Agilent Technologies, USA) operated at 30°C. The mobile phase flowing at 0.8 mL/min was 25% methanol (CH_3OH, HPLC grade, Fischer Scientific, USA) and 75% ultrapure water. The wavelength detection of acetaminophen was 243 nm. The limits of detection and quantification for this study at 95% confidence level were 5.18 and 15.69 mg/mL, respectively. The acetaminophen removal efficiency (R, %) and adsorption capacity (q_e, mg/g) were calculated by Eqs. (1) and (2):

$$R\ (\%) = \left[1 - \left(\frac{C_e}{C_o}\right)\right] \times 100\% \tag{1}$$

$$q_e\ (mg/g) = \frac{(C_o - C_e)V}{m} \tag{2}$$

where C_e (mg/L) is the equilibrium acetaminophen concentration, C_o (mg/L) is the initial acetaminophen concentration, V (L) is the solution volume and m (g) is the mass of adsorbent.

1.4. Regeneration experiments

The reusability of the 3D MnO_2/rGO was examined by conducting consecutively four adsorption-desorption cycles. The initial adsorption was carried out by agitating 30 mg of 3D MnO_2/rGO in 50 mL acetaminophen solution (20 mg/L) for 240 min and at 30°C. Then, the acetaminophen-loaded 3D MnO_2/rGO sponges were rinsed with ultrapure water to remove any loose acetaminophen residue. Acetone (C_3H_6O, 50 mL, Fischer Scientific, USA) was added to the spent adsorbent and the mixture was agitated for 240 min to desorb the pharmaceutical. The desorbed 3D MnO_2/rGO was subsequently rinsed with ultrapure water and reused in further adsorption tests.

The regeneration efficiency (η, %) and loss in adsorption capacity (q_{eL}, %) are expressed by Eqs. (3) and (4), respectively.

$$\eta = \left(\frac{q_{e,n}}{q_{e,o}}\right) \times 100\% \tag{3}$$

$$q_{eL} = \left(\frac{q_{e,n} - q_{e,n+1}}{q_{e,n}}\right) \times 100\% \tag{4}$$

where $q_{e,o}$ (mg/g) is the adsorption capacity of the initial adsorption cycle, $q_{e,n}$ (mg/g) is the adsorption capacity of the nth adsorption cycle and $q_{e,n+1}$ (mg/g) is the adsorption capacity of the $n+1^{th}$ adsorption cycle.

1.5. Adsorption modelling

The adsorption isotherm data were regressed to different isotherm models such as the Langmuir, Freundlich, Temkin and Dubinin-Radushkevich (DR) models to determine the
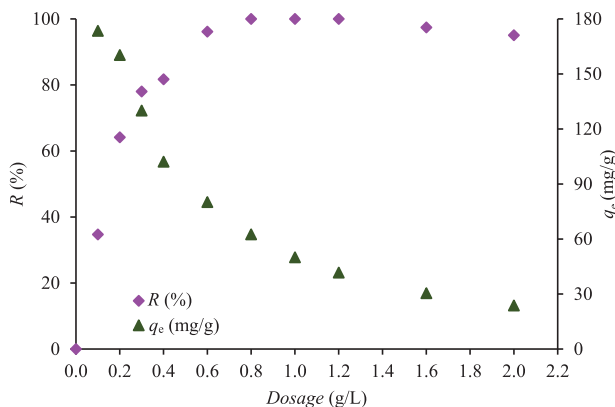
Fig. 1 – Acetaminophen removal efficiency and adsorption capacity of 3D MnO$_2$/rGO hybrid aerogel at different dosages (Acetaminophen concentration=50 mg/mL, initial pH=6.2, temperature=30°C and contact time=4 hr).
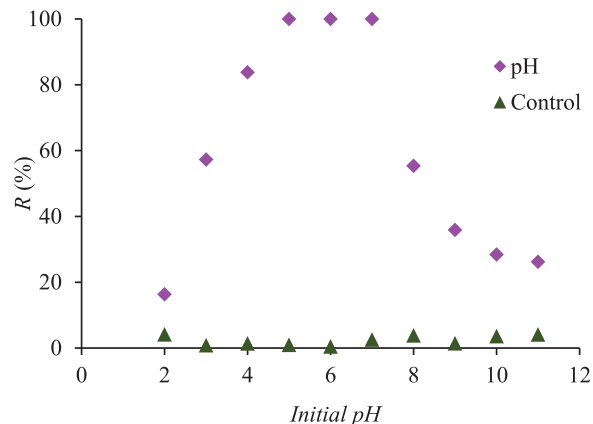
Fig. 2 – Acetaminophen removal efficiency by 3D MnO$_2$/rGO hybrid aerogel at different initial pH (Acetaminophen concentration=50 mg/mL, aerogel dosage=0.6 g/L, temperature=30°C and contact time=4 hr).

best model to describe the equilibrium behaviour of the acetaminophen-3D MnO$_2$/rGO system. The adsorption kinetic data were fitted to the Elovich, pseudo-first-order and pseudo-second-order kinetic models. The rate limiting step of the process was determined by correlating the kinetic data with the intraparticle diffusion correlation. The expressions for the adsorption equilibrium and kinetic models are presented in **Appendix A Table S1**. The parameters of the models were estimated by non-linear regression method, whereby the accuracy of the model fitting was assessed by R^2.

The thermodynamic properties such as enthalpy change (ΔH, kJ/mol), Gibbs free energy change (ΔG, kJ/mol) and entropy change (ΔS, kJ/mol K) for the investigated system were evaluated by Eqs. (5) to (7):

$$\Delta G = \Delta H - T\Delta S \tag{5}$$

$$\ln K = \frac{\Delta S}{R} - \frac{\Delta H}{RT} \tag{6}$$

$$K = \frac{q_e}{C_e} \tag{7}$$

where K is the equilibrium constant, R (J/mol K) is the ideal gas constant (J/mol K) and T (K) is the temperature. The ΔH and ΔS were evaluated based on the ΔG versus T plot.

2. Results and discussion

2.1. Adsorption attributes of 3D MnO$_2$/rGO

2.1.1. Effect of 3D MnO$_2$/rGO dosage
Fig. 1 illustrates that the acetaminophen removal efficiency increased from 34.7 to 96.1% as the 3D MnO$_2$/rGO dosage was increased from 0.1 to 0.6 g/L and it reached 100% between dosages of 0.8 – 1.2 g/L before dropping to 95% as the dosage was further increased to 2 g/L. On the other hand, the adsorption capacity exhibited a decreasing trend with the increase in 3D MnO$_2$/rGO dosage. The result was due to the availability

of a larger amount of sorption sites at higher dosage, allowing more acetaminophen to be adsorbed. However, particle agglomeration occurred at excessively large dosages which extended the diffusional pathway in the 3D MnO$_2$/rGO, thus resulting in the decrease in the removal efficiency (Wong et al., 2018). From this study, 0.6 g/L was the optimum dosage as relatively high removal efficiency (96.13%) and adsorption capacity (80.11 mg/g) were attained at this condition. To prevent agglomeration in wastewater treatment, the optimum dosage should be applied.

2.1.2. Effects of initial pH
Initial pH is a vital process parameter influencing the adsorbent surface charge, chemistry of the acetaminophen and mechanism of the separation process. The PZC of the 3D MnO$_2$/rGO aerogel, representing the pH for a neutral charge on the aerogel surface, was found to be 6.5. This implied that the adsorbent surface was positively charged at pH < 6.5 due to protonation, while deprotonation occurred at pH > 6.5 forming a negatively charged surface.

The effect of pH on the removal of acetaminophen by the 3D MnO$_2$/rGO aerogel is depicted in **Fig. 2**. It was observed that the removal percentage increased drastically from 16.34% to 100%, and remained nearly constant between pH 5 to 7, but thereafter it started to decline exponentially to 26.23% at pH 11. At very low pH of 2, the binding sites on the hybrid aerogel were protonated, causing them to have minimum interaction with the neutrally charged acetaminophen molecules. It is noteworthy that acetaminophen has an acid dissociation constant (pKa) of 9.38, enabling it to exist as a neutral molecule at pH < 9.38, whereas at pH > 9.38, it occurs as a negatively charged ion (Alfred et al., 2021).

It was observed that the 3D MnO$_2$/rGO structure disintegrated at extremely acidic condition (pH 2), damaging the sorption sites and consequently resulting in the low acetaminophen removal. As the pH was increased to 7, the adsorbent structure gained stability, whereby the active sites facilitated the uptake of acetaminophen. The exponential decline in removal efficiency after pH ~ 7 could be linked

to the adsorbent surface becoming more negatively charged (PZC=6.5), rendering it unfavourable for adsorption due electrostatic repulsion between the negatively charge adsorbent surface and negative acetaminophen ion.

The natural pH of acetaminophen solution is approximately pH 6.2, and at this pH, the 3D MnO_2/rGO aerogel was positively charged based on the PZC result, favouring the sorption of acetaminophen anions. Furthermore, at this pH, the acetaminophen removal percentage was comparatively high, as indicated by **Fig. 2**. The control plot (without the use of adsorbent) shown in **Fig. 2** reveals that the removal of acetaminophen was not affected by altering only the pH of the solution. This finding indicated that acetaminophen did not react with the surrounding chemicals in this study and its removal was solely due to adsorption phenomena. Hence, the solution pH selected for subsequent experiments was the natural pH of acetaminophen solution (∼pH 6.2). Adsorptive separation carried out at the natural pH of acetaminophen solution is highly desirable from an economic perspective as chemicals are not needed for tuning the pH of the wastewater prior to treatment.

2.1.3. Effects of acetaminophen concentration and temperature

The 3D MnO_2/rGO adsorption capacity as a function of acetaminophen concentration at increasing temperature (30 – 40°C) is illustrated in **Fig. 3**. The adsorption capacity was increased when the initial acetaminophen concentration increased. This trend was due to the higher concentration gradient providing a larger driving force for mass transfer. The higher mass transfer driving force would reduce the mass transfer resistance at the solid-liquid boundary, thereby enabling more acetaminophen to be diffused into the binding sites of 3D MnO_2/rGO. Interestingly, the adsorption capacity exhibited a positive interaction with temperature as shown by the increasing adsorption capacity (176.93 – 243.20 mg/g) as the temperature was increased from 30 to 40°C. This implied that acetaminophen adsorption onto 3D MnO_2/rGO hybrid aerogel was an endothermic process. At higher temperatures, the frequency of collision between the acetaminophen molecules with the adsorbent surface increased, hence enabling the pharmaceutical to diffuse easily into the binding sites on the 3D MnO_2/rGO structure (Yildirim & Bulut, 2020).

2.1.4. Effect of contact time

The influence of contact time and adsorption kinetic model fittings are depicted in **Fig. 4a**. At low acetaminophen concentrations (10 – 50 mg/L), the adsorption capacity increased rapidly from time, $t = 0$ till $t = 30$ min and attained equilibrium at $t > 30$ min. Meanwhile, at high concentrations (100 – 500 mg/L), a rapid increase in the adsorption capacity was observed from $t = 0$ till $t = 60$ min due to the availability of copious sorption sites at the beginning of the adsorption process (Natarajan et al., 2021). As time progressed, the adsorption sites of the 3D MnO_2/rGO aerogel were gradually saturated as demonstrated by the slower adsorption rate at $t = 60$ – 180 min, and eventually attained equilibrium state at $t > 180$ min. Notably, the adsorption capacity at equilibrium increased with enhanced concentration. This could be explained by the
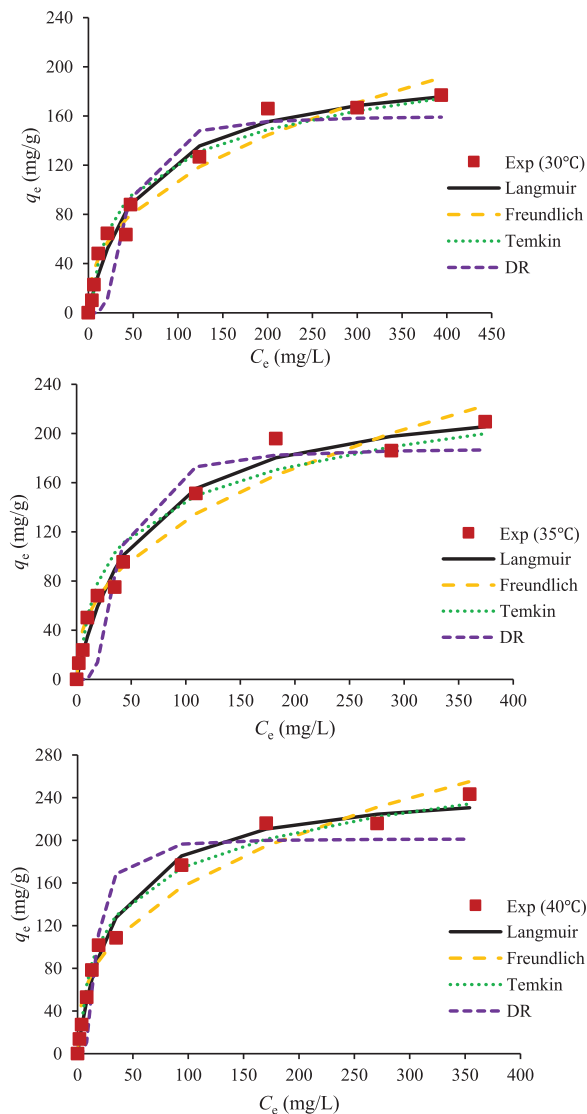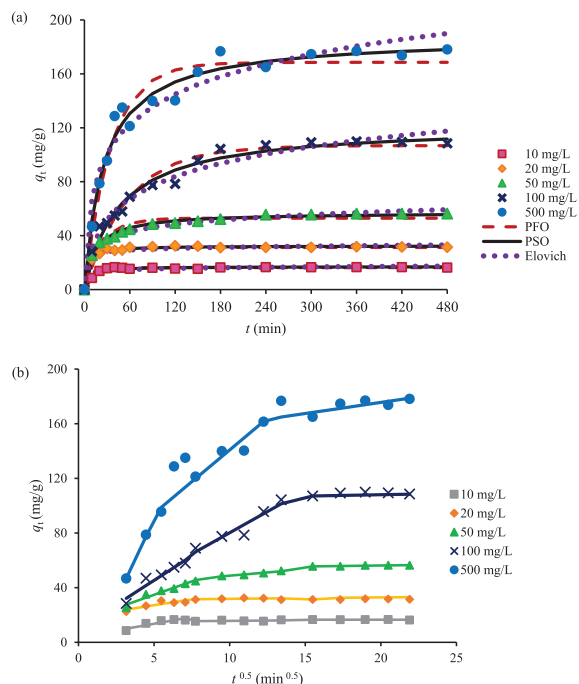

Fig. 3 – Comparison of observed adsorption equilibrium data with the Langmuir, Freundlich, Temkin and DR predictions at various temperatures (Acetaminophen concentrations=10–500 mg/mL, initial pH=6.2, aerogel dosage=0.6 g/L and contact time=4 hr).

increase in mass transfer driving force for acetaminophen transfer from the bulk liquid to the 3D MnO_2/rGO surface.

2.2. Adsorption equilibrium modelling

The adsorption equilibrium data enables the determination of the maximum adsorption capacity of the 3D MnO_2/rGO aerogel for acetaminophen. The experimental data were regressed to various isotherm models, including the Temkin, Langmuir, Freundlich and DR models. The isotherm plots are displayed in **Fig. 3** and the associated equilibrium parameters are listed in **Appendix A Table S2**. The results clearly showed that the Langmuir was the best model to describe the adsorption equilibrium with R^2 closest to unity (0.9769 – 0.9880), followed by the Temkin (0.9659 – 0.9854), Freundlich (0.9656 – 0.9688) and DR (0.8630 – 0.8916) models. This implied that the binding sites

Fig. 4 – (a) Comparison of observed adsorption kinetic data with the pseudo-first-order, pseudo-second-order and Elovich predictions, and (b) intraparticle diffusion profiles of 3D MnO$_2$/rGO at different acetaminophen concentrations (Initial pH=6.2, aerogel dosage=0.6 g/L and temperature=30°C).

were uniformly distributed on the 3D MnO$_2$/rGO surface and monolayer adsorption of acetaminophen occurred on these sites. The maximum adsorption capacity (q_m) predicted by the Langmuir model varied between 203.12 and 252.87 mg/g, while the Langmuir constant (K_L) varied between 0.0162 and 0.0292 L/mg over the temperature range studied (30 – 40°C). Furthermore, the adsorption favourability was examined by the Hall separation factor (R_L). The calculated R_L values for acetaminophen adsorption onto the 3D MnO$_2$/rGO fell within 0 – 1 (0.0641 $\leq R_L \leq$ 0.1097) indicating that the process was favourable at all investigated temperatures (Hall et al., 1966).

2.3. Adsorption kinetic modelling

The adsorption kinetic modelling provides insights into the rate of acetaminophen adsorption and the plausible rate limiting step. The kinetic model (pseudo-first-order, pseudo-second-order and Elovich) parameters are displayed in **Appendix A Table S2**. At the initial concentration C_o = 10 mg/L, the pseudo-first-order kinetic was the best fit model (R^2 = 0.9841) while the pseudo-second-order kinetic was the best kinetic model to describe the adsorption kinetic at C_o = 20 – 500 mg/L, as evident by the highest R^2 (0.9775 – 0.99). Therefore, the kinetic modelling suggested that the acetaminophen adsorption onto the 3D MnO$_2$/rGO was controlled by both physisorption and chemisorption depending on the initial concentration.

The rate limiting step of the system was identified by fitting the experimental kinetic data with the intraparticle dif-

fusion model. Generally, the uptake of acetaminophen from bulk solution is controlled by three steps: film diffusion (or boundary layer), intraparticle (or pore) diffusion and surface adsorption. As shown in **Fig. 4b**, the intraparticle diffusion plots demonstrated multi-linearity, not intercepting the origin. The trends implied that the adsorption of acetaminophen on the 3D MnO$_2$/rGO depended on several rate limiting steps such as film diffusion and intraparticle diffusion (Weber and Morris, 1963).
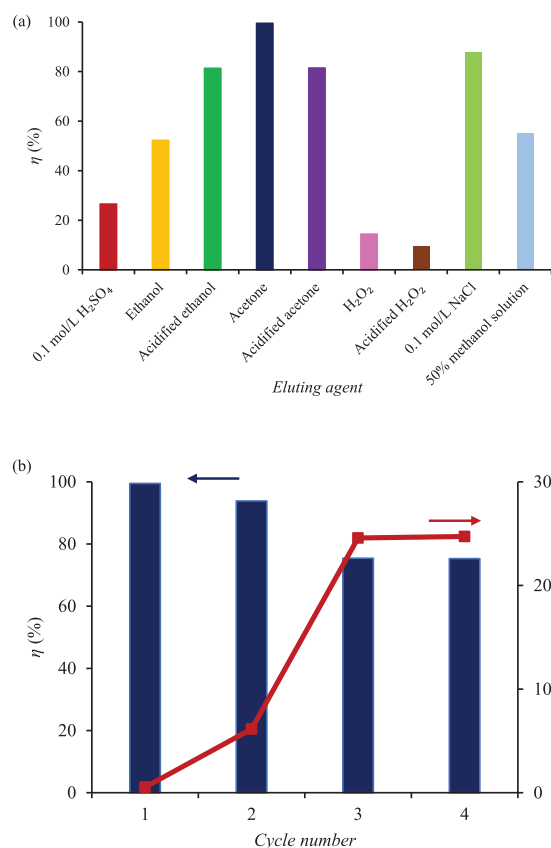
2.4. Adsorption thermodynamics

The thermodynamic parameters are summarised in **Appendix A Table S2**. Overall, the values of ΔG (-23.36 to -15.39 kJ/mol) were determined to be negative for all the temperatures and initial concentrations investigated, indicating the adsorption was thermodynamically spontaneous and feasible. Furthermore, as the temperature was increased, the ΔG decreased. It was also observed that ΔG increased with increasing concentration. These results suggested that acetaminophen adsorption was more spontaneous at high temperature and low concentration conditions. The positive ΔH (28.51 – 99.36 kJ/mol) proposed that the acetaminophen adsorption was an endothermic process, while the positive ΔS (0.1466 – 0.3880 kJ/mol K) was due to the increase in degree of randomness at the solid-liquid interface during the adsorption process.

2.5. Regeneration study

In order to determine the reusability of the exhausted 3D MnO$_2$/rGO adsorbent, a regeneration study was carried out. Different chemicals were investigated to identify the potential eluting agent for acetaminophen desorption from the spent aerogel. As observed in **Fig. 5a**, acetone had the highest regeneration efficiency (η = 99.47%) after the first regeneration cycle, followed by 0.1 mol/L NaCl (87.64%), acidified acetone (81.43%), acidified ethanol (81.31%), 50% methanol solution (55.19%), ethanol (52.26%), 0.1 mol/L H$_2$SO$_4$ (26.55%), H$_2$O$_2$ (14.40%) and acidified H$_2$O$_2$ (9.30%). Therefore, acetone was selected as the most suitable eluting agent for further regeneration experiments.
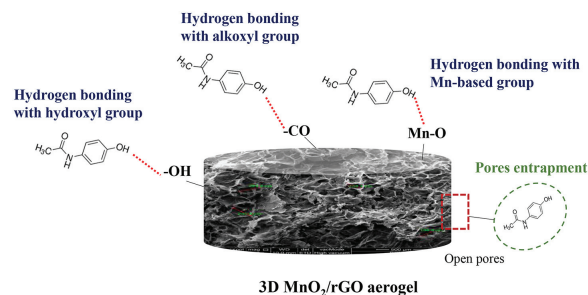
The subsequent regeneration of 3D MnO$_2$/rGO with acetone was performed for four cycles of adsorption-desorption and the results are illustrated in **Fig. 5b**. In general, the regeneration efficiency (η) was observed to decrease with an increase in the adsorption capacity loss (q_{eL}) and cycle number. The η was observed to exhibit promising efficiency (93.85% – 99.47%) during the first two cycles, then it decreased and was maintained at approximately 75% during the 3rd and 4th cycles. Furthermore, the q_{eL} progressively increased from 0.53% to 24.73 % as more adsorption-desorption cycles were conducted. This could be explained by the accumulation of chemically adsorbed acetaminophen on the adsorbent surface leading to incomplete elution. The current study revealed that the acetaminophen-loaded 3D MnO$_2$/rGO was successfully regenerated using acetone and the regeneration efficiency was maintained above 75 % even after four operating cycles.

Fig. 6 – Proposed mechanisms of acetaminophen adsorption onto 3D MnO$_2$/rGO hybrid aerogel.

Fig. 5 – (a) Regeneration efficiency of different eluting agents and (b) cyclic regeneration efficiency of 3D MnO$_2$/rGO aerogel using acetone eluent.

2.6. Adsorption mechanisms evaluation

The underlying mechanisms for the adsorption of acetaminophen onto the 3D MnO$_2$/rGO adsorbent were evaluated by several characterisation studies. Firstly, the morphology of the adsorbent was examined by FESEM and the outcomes are displayed in **Appendix A Fig. S1a – c**. The surface of the 3D MnO$_2$/rGO aerogel was interconnected by smooth wrinkled lamellar layers, forming a porous structure (**Appendix A Fig. S1a**). Furthermore, there was no agglomeration observed on the aerogel surface indicating CS had bonded onto the active sites of GO without damaging the internal structure of GO. The pore diameters were estimated to vary within 138.4 – 235.3 μm. The atomic percentage of carbon (C), oxygen (O), potassium (K) and Mn elements were 35.16, 49.31, 0.81 and 14.73%, respectively, according to the EDX results. The results confirmed the Mn element originated from the MnO$_2$. Upon inspection at higher magnification (x5000, **Appendix A Fig. S1b**), the 3D MnO$_2$/rGO surface was embellished by clusters of MnO$_2$ nanoparticles with diameters of 344.8 – 493.8 nm (**Appendix A Fig. S1c**). The deposited MnO$_2$ exhibited a ball-like structure, indicating that the MnO$_2$ could be in the δ-phase (Liu et al., 2019). Furthermore, the aggregated MnO$_2$ nanoparticles formed a platelet-like structure across the wall of the aerogel. The results revealed that the 3D MnO$_2$/rGO consisted of various pore sizes and its surface was decorated by spherical MnO$_2$ which might facilitate the adsorption of acetaminophen. The porous structure of 3D MnO$_2$/rGO could contribute towards the acetaminophen sorption via pore entrapment mechanism. The pores of the adsorbent enhanced the transportation of acetaminophen to the vacant sites within the inner part of the adsorbent, thus maximising the occupation of active sites and increasing the adsorption capacity.

The surface functional groups on the GO, pure 3D MnO$_2$/rGO and acetaminophen-loaded aerogel were identified by FT-IR, and their respective spectra are depicted in **Appendix A Fig. S1d**. The GO spectrum manifested characteristic peaks at 3446 (O-H stretch), 1622 (O-H stretch), 1373 (C-O stretch) and 1031 cm^{-1} (C-O stretch), indicating the presence of hydroxyl, carboxyl and alkoxyl functional groups on the GO nanosheets. By comparing the GO and 3D MnO$_2$/rGO spectra, the intensities of the peaks at 3446, 1622 and 1031 cm^{-1} were significantly reduced. This was a consequence of the partial removal of the oxygen functional groups of GO during the thermal reduction process. As shown in **Appendix A Fig. S1d**, the 3D MnO$_2$/rGO spectrum had peaks at 3203, 2880, 1572, 1415, 1325 and 1020 cm^{-1} referring to the O-H bonds stretching, C-H bonds stretching, -COO$^-$ groups stretching, C=O stretching vibration, O-H groups vibration bending and C-O stretch from alkoxyl group, respectively (Coates, 2000). Furthermore, the characteristic peaks at 716 and 499 cm^{-1} represented the assignment of Mn-O stretching vibration and the identification of MnO$_2$ birnessite structure on the 3D MnO$_2$/rGO (Baruah & Kumar, 2018). This finding confirmed the successful incorporation of MnO$_2$ into the aerogel which might increase its surface functionality. Notably, the FTIR spectrum of the acetaminophen-loaded 3D MnO$_2$/rGO displayed significant peak shifts from 3203, 1020, 716 and 499 cm^{-1} peaks to 3176, 1030, 720 and 496 cm^{-1}, respectively, as well as lower peaks intensities as compared to the 3D MnO$_2$/rGO spectrum. The shifts suggested the participation of the oxygen-containing (mainly hydroxyl and alkoxyl) and Mn-based functional groups of 3D MnO$_2$/rGO in adsorbing acetaminophen through hydrogen bonding, as demonstrated in **Appendix A Fig. S1d**.

The adsorption mechanisms of acetaminophen-3D MnO$_2$/rGO system were also evaluated based on the pH study. As shown in **Fig. 2**, the percentage removal of acetaminophen increased with increasing pH till pH 5. The increase in removal efficiency could be due to the involve-

Table 1 – Comparison of acetaminophen adsorption capacity by 3D MnO$_2$/rGO hybrid aerogel with other adsorbents.

Adsorbents	q_m (mg/g)	Reference
KOH-activated carbon from Jatoba fruits	356.22	(Spessato et al., 2019)
KOH-H$_3$PO$_4$ activated carbon from oak acorn	45.45	(Nourmoradi et al., 2018)
ZnCl$_2$-activated carbon from Brazil nutshells	411	(Lima et al., 2019)
H$_3$PO$_4$ activated carbon from spent tea leaves	59.2	(Wong et al., 2018)
Magnetic β-cyclodextrin polymer	128.9	(Shi et al., 2019)
Fe/N-CNT/ β-cyclodextrin nanocomposites	75.2	(Mphahlele et al., 2015)
Silica microspheres	89	(Natarajan et al., 2021)
Ca(II)-doped chitosan/β-cyclodextrin composite	200.86	(Rahman & Nasir, 2020)
Banana peel biochar	57.3	(Patel et al., 2021)
Graphene nanoplatelet C300	56.21	(Rosli et al., 2021)
CNT-COOH/MnO$_2$/Fe$_3$O$_4$ nanocomposite	80.65	(Lung et al., 2021)
3D MnO$_2$/rGO	252.87	Current study

ment of hydrogen bonding between the acetaminophen and the oxygen-containing functional groups of the 3D MnO$_2$/rGO aerogel, as well as interaction with the Mn-based functional groups, as supported by the above FTIR results. The near constant and high removal efficiency trend at pH 5 – 7 (**Fig. 2**) further suggested that other mechanisms might be involved in the adsorption of acetaminophen other than hydrogen bonding. The involvement of electrostatic interactions is excluded as acetaminophen existed in a neutral form at pH lower than its pKa (9.38).

From the discussion above, the proposed mechanisms for the adsorption of acetaminophen onto the 3D MnO$_2$/rGO hybrid aerogel such as hydrogen bonding with hydroxyl, alkoxyl and Mn-based functional groups as well as pore entrapment are depicted in **Fig. 6**.

2.7. Comparison of 3D MnO$_2$/rGO adsorption performance

The adsorption performance of 3D MnO$_2$/rGO hybrid aerogel was compared with other adsorbents such as activated carbons, biochar, magnetic β-cyclodextrin polymer, CNT based nanocomposites and silica microspheres in **Table 1**. Generally, the 3D MnO$_2$/rGO hybrid aerogel exhibited relatively high adsorption capacity towards acetaminophen. The advantages of the as-prepared 3D MnO$_2$/rGO hybrid aerogel over other reported absorbents include highly porous network, abundant oxygenated functional groups, and the presence of MnO$_2$ nanoparticles within the adsorbent. These unique features have been demonstrated to assist in the uptake of acetaminophen. The results indicated that 3D MnO$_2$/rGO hybrid aerogel is a potential adsorbent for the treatment of acetaminophen residue in wastewater.

3. Conclusions

A 3D reduced GO aerogel implanted with MnO$_2$ (3D MnO$_2$/rGO) was synthesised for the adsorption of acetaminophen. The aerogel was mesoporous and rich in oxygen-containing functional groups. Furthermore, the adsorption equilibrium of acetaminophen onto the aerogel was best described by the Langmuir model. The best adsorption kinetic model for the process was the pseudo-first-order at low concentration range,

while the pseudo-second-order was best at high concentration range. Additionally, the adsorption process was controlled by several rate limiting steps such as film diffusion and intraparticle diffusion. The mechanisms responsible for acetaminophen adsorption were identified to be hydrogen bonding with hydroxyl, alkoxyl and Mn-based functional groups in the 3D MnO$_2$/rGO hybrid aerogel, as well as pore entrapment mechanism. Thermodynamically, acetaminophen was spontaneously and endothermically adsorbed onto the 3D MnO$_2$/rGO aerogel (-23.36 $\leq \Delta G \leq$ -15.39 kJ/mol and 28.51 $\leq \Delta H \leq$ 99.36 kJ/mol). Moreover, the aerogel could be regenerated by acetone up to four consecutive adsorption and desorption cycles, with a regeneration efficiency of greater than 75%. On the whole, the study demonstrated that the 3D MnO$_2$/rGO aerogel could be used as an effective graphene-based adsorbent for acetaminophen sequestration.

Appendix A Supplementary data

Supplementary material associated with this article can be found, in the online version, at doi:10.1016/j.jes.2021.12.036.

REFERENCES

Akpotu, S.O., Moodley, B., 2018. Application of as-synthesised MCM-41 and MCM-41 wrapped with reduced graphene oxide/graphene oxide in the remediation of acetaminophen and aspirin from aqueous system. J. Environ. Manage. 209, 205–215.

Alfred, M.O., Moodley, R., Oladoja, N.A., Omorogie, M.O., Adeyemi, O.G., Olorunnisola, D., et al., 2021. Sunlight-active Cu/Fe@ZnWO4-kaolinite composites for degradation of acetaminophen, ampicillin and sulfamethoxazole in water. Ceram. Int. 47 (13), 19220–19233.

Baruah, B., Kumar, A., 2018. PEDOT:PSS/MnO2/rGO ternary nanocomposite based anode catalyst for enhanced electrocatalytic activity of methanol oxidation for direct methanol fuel cell. Synthetic Met 245, 74–86.

Coates, J., 2000. Interpretation of Infrared Spectra, a Practical Approach. Citeseer.

Dan, H., Li, N., Xu, X., Gao, Y., Huang, Y., Akram, M., et al., 2020. Mechanism of sonication time on structure and adsorption properties of 3D peanut shell/graphene oxide aerogel. Sci. Total Environ. 739, 139983.

Gabris, M.A., Rezania, S., Rafieizonooz, M., Khankhaje, E., Devanesan, S., AlSalhi, M.S., et al., 2021. Chitosan magnetic graphene grafted polyaniline doped with cobalt oxide for removal of Arsenic(V) from water. Environ. Res., 112209.

Hall, K.R., Eagleton, L.C., Acrivos, A., Vermeulen, T., 1966. Pore- and Solid-Diffusion Kinetics in Fixed-Bed Adsorption under Constant-Pattern Conditions. Ind. Eng. Chem. Fund. 5 (2), 212–223.

Hu, C.Y., Kuan, W.H., Lee, I.J., Liu, Y.J., 2021. pH-Dependent mechanisms and kinetics of the removal of acetaminophen by manganese dioxide. J. Environ. Chem. Eng. 9 (2), 105129.

Jiang, S., Yu, T., Xia, R., Wang, X., Gao, M., 2019. Realization of super high adsorption capability of 2D δ-MnO2 /GO through intra-particle diffusion. Mat. Chem. Phys. 232, 374–381.

Kekes, T., Nika, M.-C., Tsopelas, F., Thomaidis, N.S., Tzia, C., 2020. Use of δ-manganese dioxide for the removal of acetaminophen from aquatic environment: Kinetic – thermodynamic analysis and transformation products identification. J. Environ. Chem. Eng. 8 (6), 104565.

Lai, K.C., Lee, L.Y., Hiew, B.Y.Z., Yang, T.C.K., Pan, G.T., Thangalazhy-Gopakumar, S., et al., 2020. Utilisation of eco-friendly and low cost 3D graphene-based composite for treatment of aqueous Reactive Black 5 dye: Characterisation, adsorption mechanism and recyclability studies. J. Taiwan Inst. Chem. Eng. 114, 57–66.

Liao, X., Zhang, C., Nan, C., Lv, Y., Fan, Z., Hu, L., 2021. Phenol driven changes onto MnO2 surface for efficient removal of methyl parathion: The role of adsorption. Chemosphere 269, 128695.

Lima, D.R., Hosseini-Bandegharaei, A., Thue, P.S., Lima, E.C., de Albuquerque, Y.R.T., dos Reis, G.S., et al., 2019. Efficient acetaminophen removal from water and hospital effluents treatment by activated carbons derived from Brazil nutshells. Colloid. Surf. A: Physicochem. Eng. Aspect. 583, 123966.

Liu, J.Q., Zhao, W., Wen, G.L., Xu, J., Chen, X., Zhang, Q., et al., 2019. Hydrothermal synthesis of well-standing δ-MnO2 nanoplatelets on nitrogen-doped reduced graphene oxide for high-performance supercapacitor. J. Alloy. Compd. 787, 309–317.

Lung, I., Soran, M.L., Stegarescu, A., Opris, O., Gutoiu, S., Leostean, C., et al., 2021. Evaluation of CNT-COOH/MnO2/Fe3O4 nanocomposite for ibuprofen and paracetamol removal from aqueous solutions. J. Hazard. Mat. 403, 123528.

Mahmoudi, E., Azizkhani, S., Mohammad, A.W., Ng, L.Y., Benamor, A., Ang, W.L., et al., 2020. Simultaneous removal of Congo red and cadmium(II) from aqueous solutions using graphene oxide–silica composite as a multifunctional adsorbent. J. Environ. Sci. 98, 151–160.

Minale, M., Guadie, A., Li, Y., Meng, Y., Wang, X., Zhao, J., 2021. Enhanced removal of oxytetracycline antibiotics from water using manganese dioxide impregnated hydrogel composite: Adsorption behavior and oxidative degradation pathways. Chemosphere 280, 130926.

Moussavi, G., Hossaini, Z., Pourakbar, M., 2016. High-rate adsorption of acetaminophen from the contaminated water onto double-oxidized graphene oxide. Chem. Eng. J. 287, 665–673.

Mphahlele, K., Onyango, M.S., Mhlanga, S.D, 2015. Adsorption of aspirin and paracetamol from aqueous solution using Fe/N-CNT/β-cyclodextrin nanocomopsites synthesized via a benign microwave assisted method. J. Environ. Chem. Eng. 3 (4), 2619–2630 Part A.

Natarajan, R., Banerjee, K., Kumar, P.S., Somanna, T., Tannani, D., Arvind, V., et al., 2021. Performance study on adsorptive removal of acetaminophen from wastewater using silica microspheres: Kinetic and isotherm studies. Chemosphere 272, 129896.

Nourmoradi, H., Moghadam, K.F., Jafari, A., Kamarehie, B., 2018. Removal of acetaminophen and ibuprofen from aqueous solutions by activated carbon derived from Quercus Brantii (Oak) acorn as a low-cost biosorbent. J. Environ. Chem. Eng. 6 (6), 6807–6815.

Paredes-Laverde, M., Salamanca, M., Silva-Agredo, J., Manrique-Losada, L., Torres-Palma, R.A., 2019. Selective removal of acetaminophen in urine with activated carbons from rice (*Oryza sativa*) and coffee (*Coffea arabica*) husk: Effect of activating agent, activation temperature and analysis of physical-chemical interactions. J. Environ. Chem. Eng. 7 (5), 103318.

Patel, M., Kumar, R., Pittman, C.U., Mohan, D., 2021. Ciprofloxacin and acetaminophen sorption onto banana peel biochars: Environmental and process parameter influences. Environ. Res. 201, 111218.

Rahman, N., Nasir, M., 2020. Effective removal of acetaminophen from aqueous solution using Ca (II)-doped chitosan/β-cyclodextrin composite. J. Mol. Liq. 301, 112454.

Ren, F., Li, Z., Tan, W.Z., Liu, X.H., Sun, Z.F., Ren, P.G., et al., 2018. Facile preparation of 3D regenerated cellulose/graphene oxide composite aerogel with high-efficiency adsorption towards methylene blue. J. Colloid Interf. Sci. 532, 58–67.

Rosli, F.A., Ahmad, H., Jumbri, K., Abdullah, A.H., Kamaruzaman, S., Fathihah Abdullah, N.A. 2021. Efficient removal of pharmaceuticals from water using graphene nanoplatelets as adsorbent. 8(1), 201076.

Shan, D., Deng, S., Li, J., Wang, H., He, C., Cagnetta, G., et al., 2017. Preparation of porous graphene oxide by chemically intercalating a rigid molecule for enhanced removal of typical pharmaceuticals. Carbon 119, 101–109.

Shi, Y., Zhang, Y., Cui, Y., Shi, J., Meng, X., Zhang, J., et al., 2019. Magnetite nanoparticles modified β-cyclodextrin PolymerCoupled with KMnO4 oxidation for adsorption and degradation of acetaminophen. Carbohyd. Polym. 222, 114972.

Spessato, L., Bedin, K.C., Cazetta, A.L., Souza, I.P.A.F., Duarte, V.A., Crespo, L.H.S., et al., 2019. KOH-super activated carbon from biomass waste: Insights into the paracetamol adsorption mechanism and thermal regeneration cycles. J. Hazard. Mat. 371, 499–505.

Taoufik, N., Elmchaouri, A., Anouar, F., Korili, S.A., Gil, A., 2019. Improvement of the adsorption properties of an activated carbon coated by titanium dioxide for the removal of emerging contaminants. J. Water Process Eng. 31, 100876.

Tortet, L., Ligner, E., Blanluet, W., Noguez, P., Marichal, C., Schäf, O., et al., 2017. Adsorptive elimination of paracetamol from physiological solutions: Interaction with MFI-type zeolite. Micropor. Mesopor. Mat. 252, 188–196.

Tyszczuk-Rotko, K., Jaworska, I., Jędruchniewicz, K., 2019. Application of unmodified boron-doped diamond electrode for determination of dopamine and paracetamol. Microchem. J. 146, 664–672.

Weber, W.J., Morris, J.C.1963, 1963. Kinetics of adsorption on carbon from solution. J. Sanit. Eng. Div. 89, 31–60.

Wong, S., Lim, Y., Ngadi, N., Mat, R., Hassan, O., Inuwa, I.M., et al., 2018. Removal of acetaminophen by activated carbon synthesized from spent tea leaves: equilibrium, kinetics and thermodynamics studies. Powder Technol. 338, 878–886.

Yanyan, L., Kurniawan, T.A., Albadarin, A.B., Walker, G., 2018. Enhanced removal of acetaminophen from synthetic wastewater using multi-walled carbon nanotubes (MWCNTs) chemically modified with NaOH, HNO3/H2SO4, ozone, and/or chitosan. J. Mol. Liq. 251, 369–377.

Yao, Q., Fan, B., Xiong, Y., Jin, C., Sun, Q., Sheng, C., 2017. 3D assembly based on 2D structure of Cellulose Nanofibril/Graphene Oxide Hybrid Aerogel for Adsorptive Removal of. Antibiotics in Water. Sci. Rep. 7, 45914.

Yildirim, A., Bulut, Y., 2020. Adsorption behaviors of malachite green by using crosslinked chitosan/polyacrylic acid/bentonite composites with different ratios. Environ. Technol. Innov. 17, 100560.

Yu, B., Bai, Y., Ming, Z., Yang, H., Chen, L., Hu, X., et al., 2017. Adsorption behaviors of tetracycline on magnetic graphene oxide sponge. Mat. Chem. Phys. 198, 283–290.

Zou, S.-J., Ding, B.-H., Chen, Y.-F., Fan, H.-T., 2021. Nanocomposites of graphene and zirconia for adsorption of organic-arsenic drugs: Performances comparison and analysis of adsorption behavior. Environ. Res. 195, 110752.